

Supplemental Digital Content 1

Materials and Methods

1.1 Oxygen-glucose deprivation

Oxygen-glucose deprivation (OGD) was achieved by superfusing the slices with glucose-free deoxygenated artificial cerebrospinal fluid (ACSF) that was equilibrated with an anaerobic gas mixture (95% N₂, 5% CO₂). During OGD the oxygen content of the superfusate was always less than 2 mm Hg, as determined by a fiber-optic system (FOXY-R probe and SF2000 Spectrofluorometer, Ocean Optics Inc., Dunedin, FL).

1.2 Perchloric Acid metabolite extraction

Perchloric acid extraction and nuclear magnetic resonance (NMR) tube loading were done as in earlier studies.¹⁻³ Lyophilized dry perchloric acid extracts were weighed and stored at – 80°C until just prior to NMR, at which time they were dissolved in D₂O containing 10 mM DSS-d₆. DCl and NaOD were used to adjust the pD into the range 7.0 to 7.2. 200 microliters was then placed in 3 mm NMR tubes (Select Series™ S-3-900-7 made of ASTM Type 1 Class A glass, specifically designed for high-resolution NMR spectroscopy, Norell Inc., Landisville, NJ)

1.3 Adenosine Triphosphate (ATP) Bioluminescence Assay

In order to validate ¹H NMR determinations of ATP levels from quantifications of the 8.510 ppm resonance that comes from the only proton on ATP's five-membered nitrogen-containing ring within adenine,⁴ a luciferin bioluminescence assay (kit HS II, Cat. No. 11 699 709 001, Roche Applied Science, Indianapolis, IN) was used to separately measure ATP levels in all perchloric acid extracts that were studied with NMR for all time points. Ratios of assay measurements for different time points were subsequently compared with ratios of the ¹H ATP signal intensities in the same extract samples. The firefly luciferase (EC 1.13.12.7) in the assay

catalyzed the oxidation of luciferin in the presence of ATP, causing green emission light at 562 nm in quantities linearly related to the ATP concentration.⁵ Immediately after preparing the neutralized extracts in D₂O for NMR analysis, a 2 μL aliquot was removed and stored at -80°C for the subsequent ATP bioluminescence assay. Final ATP concentrations for each sample were obtained by averaging two duplicate quantifications.

1.4 Glial Fibrillary Acidic Protein (GFAP) immunohistochemistry

Immunohistochemistry was used to assess rapid upregulation of the synthesis of GFAP, a major cytoskeletal intermediate filament protein important to astrocyte motility and structural stability, and a well known biomarker for central nervous system reaction to injury, chemical insults, and inflammation,^{6,7} despite the existence of substantial numbers of GFAP-negative protoplasmic astrocytes in gray matter structures, including the cerebral cortex.⁸ Three slices from both the Hypothermia and Normothermia groups were removed at T₀ and T₃, and fixed overnight at 4°C in freshly made 4% formaldehyde. After cryoprotection, slices were cut into 10 μm thick sections on a cryostat (Leica, CM1900, Solms, Germany). Sections were processed for fluorescence GFAP immunohistochemistry with 1:1000 diluted mouse monoclonal anti-GFAP conjugated to Cy3 reactive dye (Sigma, C9205, Sigma-Aldrich, St. Louis, MO). A Zeiss Axioskop Fluorescence Microscope (Thornwood, NY) with a 510-550 nm excitation wavelength window and 570 nm emission wavelength detection was used at 200X magnification to obtain photomicrographs of stained coronal sections. Quantifications of relative optical densities of immunostaining indicating intensities of GFAP immunoreactivity was quantified with National Institutes of Health (Bethesda, MD) public domain program ImageJ by observers blinded to experimental information. Statistical comparisons were done with JMP ANOVA software (SAS Institute Inc., Cary, NC).

1.5 NMR data acquisition and analysis

NMR data were obtained at the Central California 900 MHz NMR Facility, which operates with National Institutes of Health support (GM68933) in the QB3 facilities at University of California-Berkeley.

1D ^{13}C spectra were acquired at 226.2 MHz on a 21.1 Tesla Bruker Avance II NMR spectrometer (Bruker Corporation, Billerica, MA) equipped with a 5 mm CPTXI multinuclear cryoprobe optimized for ^{13}C . Data were collected using a 30° tip angle pulse followed by the collection of 64 K data points with a spectral width of 250 ppm. ^1H decoupling was used during the acquisition time of 0.58 s and the recycle delay was set to 2.0 s. A total of 12K scans were signal averaged, and each experiment was recorded in 9 h. Correction factors for ^{13}C NOE enhancements and spin relaxation were obtained from special sequential runs having recycle delays of 2 s and 90 s.

1D ^1H spectra were acquired at 900 MHz using a 30° tip angle pulse with 128 K points over 4.65 s and with a recycle delay of 1.0 s, for a total interexperiment delay of 5.65 s. Solvent suppression was not used. Because of power tolerance limitations of the cryoprobe, with the parameters just mentioned it was not possible during ^1H acquisitions to have broadband ^{13}C -decoupling across the 200 ppm ^{13}C range with metabolite resonances. ^1H spectra were processed without apodization or zero filling and were referenced to 4,4-dimethyl—silapentane-1-sulfonic acid (DSS). Linewidths of DSS's methyl resonances typically ranged from 1.0 to 1.5 Hz (0.0011 to 0.0017 ppm). Checks on ^1H resonance assignments and quantifications were done by acquiring *Two-Dimensional (2D) ^1H J-resolved NMR* spectra and then obtaining one dimensional (1D) projections along the ^1H axis (1D ^1H pJRES spectra), so as to greatly eliminate the J-J coupling and considerably reduce resonance peak overlap. 2D J-Resolved spectra were recorded with a single echo experiment,⁹⁻¹¹ using pulse parameters described

elsewhere.¹¹

NMR metabolites corresponding to different chemical shifts were identified and preprocessed with Bruker software (TopSpin 3.1 and AMIX, Bruker Corporation), and quantified with iNMR[®] (Nucleomatica, Molfetta, Italy). Chemical shift assignments were checked against published values^{4,12} and metabolomics data bases.¹³⁻¹⁶ Relaxation corrections were derived from a special set of runs. The same NMR pulse sequence was used for all runs, and metabolite differences were measured relative to control values. Metabolite signal intensities were computed relative to DSS and normalized to both the weight of the dry powder and the total spectral area. The total ¹H and ¹³C spectral areas (excluding the water peak in ¹H data) were also compared to the 10 mM DSS signal intensity, and to an upfield Bruker-generated resonance signal with area equivalent to 20 mM (the ERETIC[™] signal intensity.)

1.6 Calculations: (pyruvate carboxylase)/(pyruvate dehydrogenase) and (acetate/glucose)

Acetate uptake is specific to glia,¹⁷ which metabolize [1,2-¹³C]acetate into [4,5-¹³C]glutamate and identically labeled glutamine. The latter is transported to neurons and converted to [4,5-¹³C]glutamate, and [1,2-¹³C]GABA.¹⁸ Glia also metabolize [1-¹³C]glucose by forming [3-¹³C]pyruvate, which enters TCA (tricarboxylic acid) cycle *via*: 1) pyruvate dehydrogenase (PDH), the major glial pathway and only one for neurons; and, 2) pyruvate carboxylase (PC).

The ratio of flux from glucose metabolized *via* PC to that metabolized *via* PDH can be estimated for both glutamate and glutamine by the formula $[C2 - C3]/C4$, where the symbols correspond to central resonance peaks alone (from isotopomer molecules having only one ¹³C), and the calculation is separate for glutamate and glutamine. This formula, well known from earlier studies,^{19,20} can be appreciated from figure 1B in the manuscript as follows. Passage *via* PDH results in a single ¹³C on the fourth carbon (C4) for α -ketoglutarate, and thus for both glutamate

and glutamine. When passage is *via* PC, a single ^{13}C label is on the second carbon (C2). Unfortunately, this is not the only way for α -ketoglutarate to end up with a single C2 label. Some of the glucose that is metabolized through PDH on the first turn, thereby obtaining a ^{13}C on C4, will undergo a second turn that generates equal amounts of single-labeled α -ketoglutarate having ^{13}C at C2 or C3. Figure 1B from the manuscript) shows that the first turn through PDH ends with the creation of equal amounts of $[2\text{-}^{13}\text{C}]\text{oxaloacetate}$ and $[3\text{-}^{13}\text{C}]\text{oxaloacetate}$. To understand the labels generated in a second turn one follows the two blue circles and sees that they end up at positions C2 and C3 of glutamate and glutamine. Thus the formula for estimating the PC/PDH ratio is $(\text{C2} - \text{C3})/\text{C4}$. In this equation numbers are for the singlet resonance peaks alone (*i.e.*, exclusive of other isotopomers). Similarly, the PC/PDH ratio for γ -aminobutyric acid is $(\text{C4} - \text{C3})/\text{C2}$. These formulae, although commonly used, are not exact, because the same isotopomers can arrive by other pathways.²¹ However such is not an issue here, because we are looking for differences among three similar experimental groups, not trying to make absolute flux measurements.

The formula for the ratio of acetate's contribution to glucose's contribution to both glutamate or glutamine production is similarly $\text{C45}/\text{C4}$. Because acetate is doubly labeled, it is transformed to $[4,5\text{-}^{13}\text{C}]\text{glutamate}$. As noted, on the first turn, ^{13}C -glucose contributes only to C4. Similarly, the acetate/glucose ratio for γ -aminobutyric acid is $\text{C12}/\text{C2}$. One does not have to be concerned with contamination from subsequent turns, as was the case in calculating PC/PDH. This is due to an interesting feature of the TCA Cycle, namely that in multiple turns *via* PDH, the methyl carbon of acetyl-CoA (C2, as in $[2\text{-}^{13}\text{C}]\text{acetyl-CoA}$) can ultimately enrich any of the carbons in glutamate except C5, whereas the carbonyl carbon of acetyl-CoA, (C1 in $[1,2\text{-}^{13}\text{C}]\text{acetyl-CoA}$) can enrich only carbons 1 or 5, and never carbons 2, 3, and 4.²²

Results: Analysis of ^1H ATP peak at $\approx 8.51\text{ppm}$

2.0 Quantifying ATP from its ^1H resonance peak at $\approx 8.51\text{ppm}$

The insert to figure 4C in the manuscript illustrates the difficulty encountered in quantifying ATP from its 8.51 ppm resonance. An unknown resonance overlapped the ATP peak, centered only ≈ 0.010 ppm to the left (downfield.) ATP identification was confirmed by adding pure ATP (Sigma-Aldrich) to the NMR tube and seeing that only the right sided peak increased. Rather than undertake further complex investigations, the issue was dealt with by deconvolution. Lorentzian fits to the two peaks at 8.510 ppm, done with iNMR. Signal intensities for the right-sided resonance were taken as the NMR quantification of ATP (henceforth denoted by “ATP- ^1H ”).

2.1 Linear Regression Analysis of ATP quantifications from ^1H NMR analysis and ATP Bioassay

Figure 1 compares bioassay quantifications of ATP (“ATP-bioassay”) with NMR quantifications of ATP (“ATP- ^1H ”) that were obtained by deconvolution, using data from all time points and treatment groups. Data points in a dotted rectangular box at the bottom left, all from T_1 (end of OGD), have final-to-initial ATP-bioassay levels below 0.1. A three degrees-of-freedom linear regression fit to the ATP data, done after excluding the low value T_1 data points, produced a regression line slope coefficient of 0.98 ($p < 1.9 \times 10^{-5}$; $R^2 = 0.71$), in support of our having used ^1H NMR for ATP determinations for all time points other than T_1 .

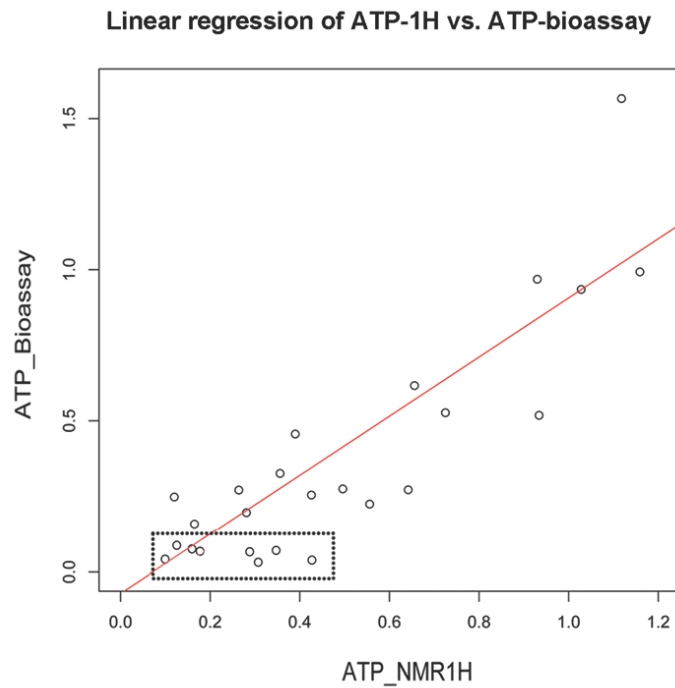


Fig. 1. Shows a comparison of ATP quantifications of the same sample by two methods discussed in the text: ATP-Bioassay (vertical axis) and ATP-1H (horizontal axis). The red line rising from the lower left is the result of a linear regression fit to points outside of the dotted box, indicating a close relation between the two types of measures. Data points in the dotted rectangular box were not included when fitting the straight line because an overlapping NMR peak made small ATP-1H quantifications unreliable, as explained in the text.

References:

1. Espanol MT, Litt L, Yang GY, Chang LH, Chan PH, James TL, Weinstein PR: Tolerance of low intracellular pH during hypercapnia by rat cortical brain slices: A $^{31}\text{P}/^1\text{H}$ NMR study. *J Neurochem* 1992; 59:1820-8
2. Liu J, Hirai K, Litt L: Fructose-1,6-bisphosphate does not preserve ATP in hypoxic-ischemic neonatal cerebrocortical slices. *Brain Res* 2008; 1238:230-8
3. Liu J, Segal M, Yoo S, Yang GY, Kelly M, James TL, Litt L: Antioxidant effect of ethyl pyruvate in respiring neonatal cerebrocortical slices after H_2O_2 stress. *Neurochem Int* 2009; 54:106-10
4. Govindaraju V, Young K, Maudsley AA: Proton NMR chemical shifts and coupling constants for brain metabolites. *NMR Biomed* 2000; 13:129-53
5. Lundin A, Richardsson A, Thore A: Continuous monitoring of ATP-converting reactions by purified firefly luciferase. *Anal Biochem* 1976; 75:611-20
6. Eng LF, Ghirnikar RS, Lee YL: Glial fibrillary acidic protein: GFAP-thirty-one years (1969-2000). *Neurochem Res* 2000; 25:1439-51
7. Qiu Y, Pan J, Li Y, Li X, Li M, Abukhousa I, Wang Y: Relationship between activated astrocytes and hypoxic cerebral tissue in a rat model of cerebral ischemia/reperfusion. *Int J Neurosci* 2011; 121:1-7
8. Giffard RG, Swanson RA: Ischemia-induced programmed cell death in astrocytes. *Glia* 2005; 50:299-306
9. Aue WP, Bartholdi E, Ernst RR: Two-dimensional spectroscopy. Application to nuclear magnetic resonance. *J Chem Phys* 1976; 64:2229-46
10. Aue WP, Karhan J, Ernst RR: Homonuclear broad band decoupling and two-dimensional J-resolved NMR spectroscopy *J Chem Phys* 1976; 64:4226-7

11. Ludwig C, Viant MR: Two-dimensional J-resolved NMR spectroscopy: Review of a key methodology in the metabolomics toolbox. *Phytochem Anal* 2010; 21:22-32
12. Willker W, Engelmann J, Brand A, Leibfritz D: Metabolite identification in cell extracts and culture media by proton-detected 2D [^1H , ^{13}C] NMR spectroscopy. *J Magn Res Anal* 1996; 2:21-32
13. Wishart DS, Tzur D, Knox C, Eisner R, Guo AC, Young N, Cheng D, Jewell K, Arndt D, Sawhney S, Fung C, Nikolai L, Lewis M, Coutouly MA, Forsythe I, Tang P, Shrivastava S, Jeroncic K, Stothard P, Amegbey G, Block D, Hau DD, Wagner J, Miniaci J, Clements M, Gebremedhin M, Guo N, Zhang Y, Duggan GE, Macinnis GD, Weljie AM, Dowlatabadi R, Bamforth F, Clive D, Greiner R, Li L, Marrie T, Sykes BD, Vogel HJ, Querengesser L: HMDB: The Human Metabolome Database. *Nucleic Acids Res* 2007; 35:D521-6
14. Cui Q, Lewis IA, Hegeman AD, Anderson ME, Li J, Schulte CF, Westler WM, Eghbalnia HR, Sussman MR, Markley JL: Metabolite identification *via* the Madison Metabolomics Consortium Database. *Nat Biotechnol* 2008; 26:162-4
15. Zhou B, Wang J, Ressom HW: MetaboSearch: Tool for mass-based metabolite identification using multiple databases. *PLoS One* 2012; 7:e40096
16. Ludwig C, Easton JM, Lodi A, Tiziani S, Manzoor SE, Andrew D, Southam AD, Byrne JJ, Bishop LM, He S, Theodoros N, Arvanitis TN, Günther UL, Viant MR: Birmingham Metabolite Library: A publicly accessible database of 1-D ^1H and 2-D ^1H J-resolved NMR spectra of authentic metabolite standards (BML-NMR). *Metabolomics* 2012; 8:8-18
17. Waniewski RA, Martin DL: Preferential utilization of acetate by astrocytes is attributable to transport. *J Neurosci* 1998; 18:5225-33
18. Kvamme E, Roberg B, Torgner IA: Glutamine transport in brain mitochondria. *Neurochem Int* 2000; 37:131-8

19. Taylor A, McLean M, Morris P, Bachelard H: Approaches to studies on neuronal/glia relationships by ^{13}C -MRS analysis. *Dev Neurosci* 1996; 18: 434-42
20. Haberg A, Qu H, Haraldseth O, Unsgard G, Sonnewald U: In vivo injection of [1- ^{13}C]glucose and [1,2- ^{13}C]acetate combined with ex vivo ^{13}C nuclear magnetic resonance spectroscopy: a novel approach to the study of middle cerebral artery occlusion in the rat. *J Cereb Blood Flow Metab* 1998; 18: 1223-32
21. Zwingmann C, Leibfritz D: Glial-Neuronal Shuttle Systems. , *Handbook of Neurochemistry and Molecular Neurobiology*, 3rd edition. Edited by Lajtha A, Gibson GE, Diener GA, Springer US, 2007, pp 197-238
22. Sherry AD, Malloy CR: Isotopomer analysis of glutamate, *Biological Magnetic Resonance*, 1 edition. Edited by Berliner LJ, Robitaille P-M, Springer-Verlag, New York, 2008, pp 87